THERMODYNAMIC ANALYSIS OF COMBUSTION EVENTS IN THE NATURAL GAS FUELLED SI ENGINE WITH VVT

Magdalena Szwaja, Paweł Mazuro

Warsaw University of Technology
Faculty of Power and Aeronautical Engineering
Nowowiejska Street 21/25, 00-665 Warsaw, Poland
e-mail: magdaszw@onet.pl, pmazuro@itc.pw.edu.pl

Stanisław Szwaja

Czestochowa University of Technology
Mechanical Engineering and Computer Science Faculty
Armii Krajowej Av. 21, 42-201 Czestochowa, Poland
e-mail: szwaja@imc.pcz.pl

Abstract

The main aim of the research was to investigate influence of overlap of the natural gas fuelled spark ignited engine on the following parameters: Indicated Mean Effective Pressure (IMEP), heat rate release including combustion phases (ignition lag, main combustion phase). The content of the study includes results from processing in-cylinder pressure measurements, heat release rate analysis, combustion phases, and finally the conclusions. The tests were carried out on the test bed including the single cylinder research engine with a displacement volume of 550 cm³. The engine was equipped with independent cam phasors for both intake and exhaust valves, but for this investigation, the exhaust valve timing was fixed (the exhaust cam centre line was fixed at -95 crank angle (CA) deg before Top Dead Centre) and intake valve timing was changed (the intake cam centre line was varied from 90 to 150 CA deg after Top Dead Centre). The overlap was changed in the range from 85 to 25 CA deg. 8 tests series were performed, each singular series consisted of 300 consecutive engine combustion cycles. As observed, by varying the valve overlap it contributes to significant change in the peak combustion pressure, peak of heat release rate, and combustion phases. Summing up, variable valve timing affects compression and expansion strokes by changing polytropic indexes due to various amounts of exhaust residuals trapped in the cylinder. It affects not only engine volumetric efficiency but also the heat release rate and IMEP, so it does engine performance. Thus, variable valve timing can be considered as valuable tool that can be applied to the natural gas fuelled internal combustion engine.

Keywords: internal combustion engine, variable valve timing, heat release rate, IMEP, combustion phases

1. Introduction

Among others, various constructions have been systematically introduced to mechanical trains in the internal combustion (IC) engine to increase its efficiency as well as to reduce toxic exhaust emissions [1-3]. Furthermore, intensive works on engine modernization is stimulated by applying various substitute fuels with respect to limited fossil fuels resources [4].

Results from experimental work presented in this article are focused on evaluating the impact of variable valve overlap on engine performance, thermodynamics of compression and expansion strokes and combustion rates in a methane fuelled spark ignited engine. However, as known from literature survey [3, 5], variable valve timing influences on several parameters which directly affect combustion rate in the engine cylinder. They are as follows: amounts and temperature of exhaust residuals, volumetric efficiency, real both compression and expansion ratio etc. Exhaust gas residuals, if considered as diluent, can affect combustion probably in similar way the EGR (external exhaust gases recirculation) or lean mixture influences on it [6, 7]. To simplify

considerations on these issues, the analysis of the primary parameter – the overlap – on combustion progress was assumed as the preliminary investigation in this field. In the next step, someone can find analytical correlation between the overlap and each of the above-mentioned parameters and conclude on their separate impact on the combustion rate. Methane was used as the fuel for tests because it can be considered as the most appropriate reference fuel for natural gas.

2. Experimental set-up

The tests were conducted on the single cylinder research engine based on Ricardo's Hydra platform. The engine specifications are provided in Tab. 1.

Tab. 1. Specifications of the single cylinder Hydra engine

Parameter	Description
Base Engine	GM Ecotec GEN II LAF
Bore	86.00 mm
Stroke	94.60 mm
Connecting rod length	152.5 mm
Wrist pin offset	0.8 mm
Displacement	0.55 dm^3
Compression Ratio	10.93:1
PFI injection	Methane
Cam Phasing	Dual independent high authority
Engine Control	Prototype for full set-point operation of throttle, fuel, spark, cams, etc.

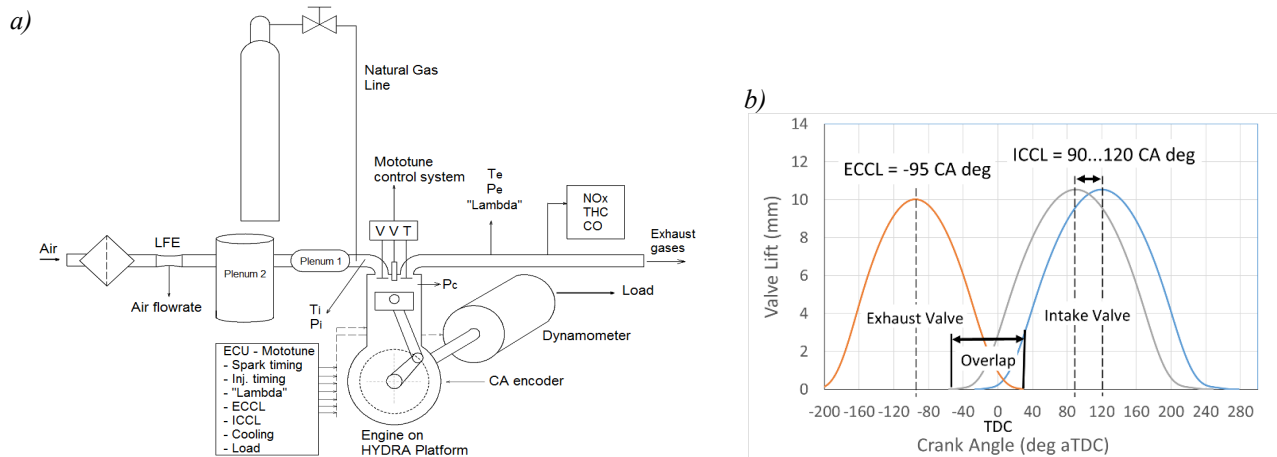The engine setup and valve lift profiles are shown in Fig. 1a.

Fig. 1. Hydra engine setup (a), intake and exhaust valve lift profiles (b)

Variable valve overlap was achieved through phasing the intake valve timing relative to a fixed exhaust valve timing. The intake valve cam centre line location (ICCL) varies from 90 to 150 crank angle (CA) deg after TDC, while the exhaust valve cam centreline location (ECCL) was fixed at 95 CA deg before TDC. The valve profiles are shown in Fig. 1b.

The valve overlap is defined as duration between intake valve opening (IVO) and exhaust valve closing (EVC). Hence, it is expressed in crank angle degrees.

All the tests were performed in the following conditions presented in Tab. 2. The spark timing for combustion events was optimized to obtain Maximum Brake Torque (MBT).

Tab. 2. Test conditions

No.	Parameter	Test 1 to 8
1	Engine speed	1250 rpm
2	Relative air to fuel ratio "lambda"	1.0 … 1.04
3	Fixed load NMEP	450 ±7 kPa
4	Fixed location for 50% fuel burnt CA50	7.2 ±0.5 CA deg
5	ECCL	-95 CA deg
6	Test No. 1 ... 8	1, 2, 3, 4, 5, 6, 7, 8
7	ICCL	150, 150, 140, 130, 120, 110, 100, 90
8	Overlap	85, 85, 75, 65, 55, 45, 35, 25

3. Results and discussion

In Fig. 2a, the in-cylinder pressure history zoomed to combustion phase is depicted. As seen, with higher overlapboth, the peak pressure and pressure at the compression stroke are lower, that is mainly due to lower amounts of gas charge filling the cylinder. Fig. 2b shows the entire p-V diagram in log scale. As observed, changes in pressure are also observed at the pumping phase with change in overlap.
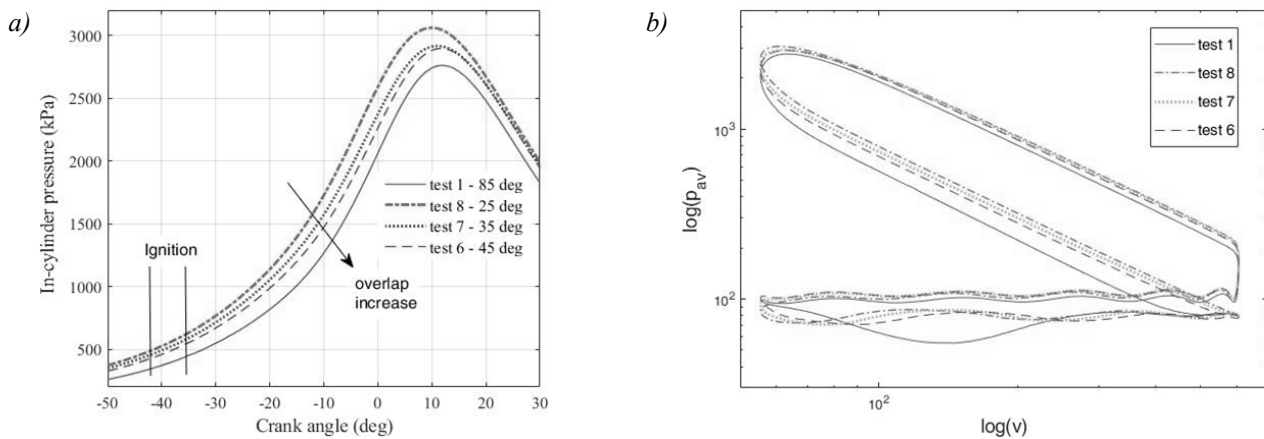

Fig. 2. In-cylinder pressure vs. crank angle for selected overlaps (a), p-V diagram in log scale (b)

Indicated mean effective pressure for the specific test series was determined as average from 300 consecutive combustion events with the equation (1):

$$IMEP = \sum \frac{\Sigma_i(p_i \cdot dV)}{V_s} / 300 , \tag{1}$$

where:
p_i – in-cylinder pressure,
dV – volume increment,
V_s – cylinder displacement.

Table 3 presents results of IMEP and COV of IMEP for each test series at fixed load of approximately 478 kPa.

For further analysis calculation of polytropic indexes for both the compression and the expansion stroke was performed. They were simply determined as coefficients in linear correlation between pressure and volume in log scale as depicted in Fig. 3a. Points for calculation were taken as follows:
– for compression process: x_1 = -62 CA deg, x_2 = -45 CA deg (at least 3 CA deg prior to the most advanced spark timing for the test series 8),

Tab. 3. IMEP Results

Test No.	IMEP (kPa)	Standard deviation of IMEP (kPa)	COV of IMEP (%)	Spark Timing (deg)
1	476.9	4.10	0.86	-35
2	473.8	4.49	0.95	-33
3	475.5	4.53	0.95	-33
4	479.7	3.96	0.83	-31
5	478.2	5.51	1.15	-31
6	481.2	6.33	1.32	-34
7	478.6	7.97	1.67	-37
8	476.1	9.72	2.04	-42
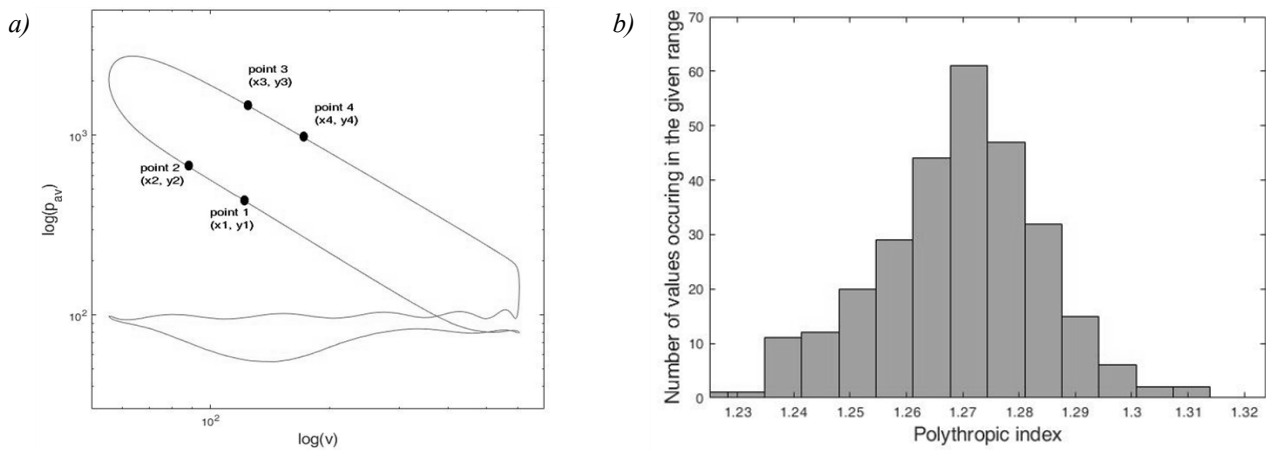
Fig. 3. Locations of reference points to calculate polytropic indexes (a), exemplary distribution of compression polytropic index from selected series consisted of 300 consecutive combustion events (b)

– for compression process: $x_3 = 60$ CA deg, $x_4 = 77$ CA deg.

Additionally, error tolerance was inserted to show accuracy of obtained results determined on the basis of Gaussian normal distribution (Fig. 3b).

Figure 4 presents correlations between these both polytropic indexes and overlap. As can be noticed, general trend line is slightly positive for both these cases. Moreover, expansion index is lower than the compression one. It is caused by two independent effects:
– higher heat transfer rate to the cooling system at the expansion stroke,
– higher percentage of tri-atomic gases (CO_2 and H_2O) in the expansion working fluid.

On the basis of these above-mentioned effects, in the same way the positive trend in both indexes vs. overlap can be explained. Higher polytropic index goes with higher amounts of exhaust gas residuals in the total in-cylinder charge and/or less intensified heat transfer rate to cylinder walls. Heat transfer rate to walls is usually in line with peak combustion temperature, so is with higher amounts of exhaust residuals, which, working as diluent, reduce combustion temperature.

Analysis of heat released from combustion

Heat release rate (HRR) from combustion was calculated from the energy conservation law with the final equation (2):

$$\frac{\mathrm{d}Q}{\mathrm{d}\Theta} = \frac{1}{k-1} V \cdot \frac{\mathrm{d}p}{\mathrm{d}\Theta} + \frac{k}{k-1} p \cdot \frac{\mathrm{d}V}{\mathrm{d}\Theta},$$ (2)

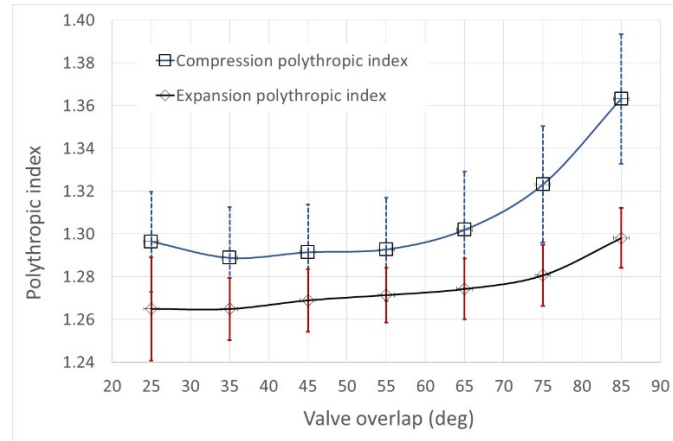where:
k – specific heat ratio ($k = c_p/c_v$),

Fig. 4. Polytropic indexes vs. overlap

dp – in-cylinder pressure increment,
dV – volume increment,
dΘ – crank angle increment.

The specific heat ratio k was determined analytically taking into account gas composition before ignition. It was assumed the *k* is constant during combustion and is nearly 1.39. Fig. 5a presents selected HRR for various overlaps. As observed, higher peak in HRR goes with higher overlap. It is also depicted in detail in Fig. 5b.
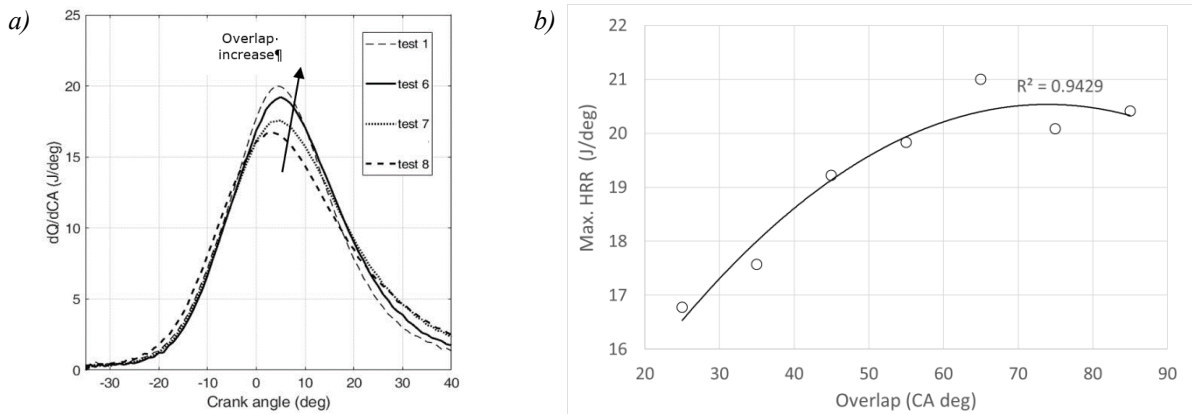

Fig. 5. Exemplary HRRs for various overlaps vs. crank angle (a), maximum of HRR vs. overlap (b)

Combustion phases CA0-10 and CA10-90 can be considered as ignition delay and main combustion phase, respectively. The combustion phase CA0-10 presents itself crank angle associated with 10% heat released starting from ignition point. Hence, CA10-90 responds crank angle for 80% cumulative heat released from 10 to 90%. These combustion phases can be easily determined from cumulative heat plot $Q(\Theta)$ (Fig. 6), which can be calculated with equation (3) by integrating equation (2):

$$Q(\Theta) = \int_{\Theta_1}^{\Theta_2} \left(\frac{dQ}{d\Theta} \right) d\Theta,$$ (3)

where:
Θ_1 – crank angle expressing start of combustion,
Θ_2 – crank angle at which HRR gets negative after combustion phase (usually 50-60 CA aTDC).

Three exemplary plots of cumulative heat Q(Θ) for various overlaps are depicted in Fig. 6. In literature, it is usually determined with empirical equations as MFB (mass fuel fraction burnt). As seen, increase in overlap leads to shorten combustion phases.
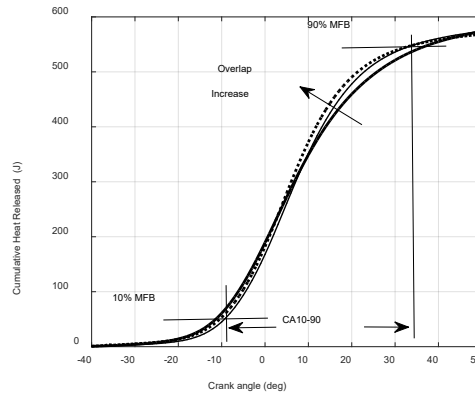
Fig. 6. Cumulative heat released from combustion for three exemplary test series with various overlaps

As plotted in Fig. 7a, the main combustion phase CA10-90 in explicit negative trend with increase in overlap. Unlike CA0-10, this phase has its minimum at overlap nearly 60-70 CA deg. Additionally, strong negative linear correlation between CA10-90 and maximum in HRR was observed (Fig. 7b). This trend was expected to be negative, as the peak in HRR is located in the main combustion phase CA10-90.
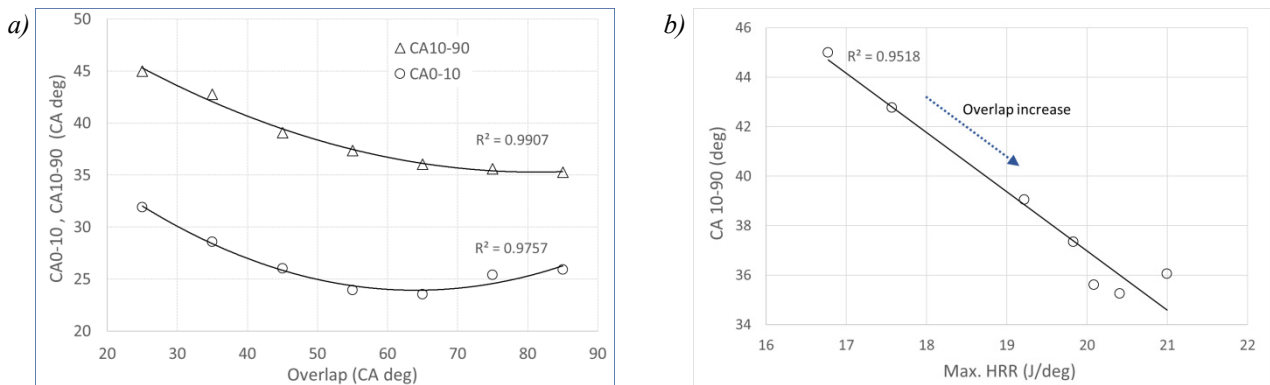

Fig. 7. Combustion phases CA0-10 and CA10-90 vs. overlap (a), main combustion phase CA10-90 vs. max. HRR with variable overlap (b)

4. Conclusions

Investigation dealt with influence of overlap on the selected thermodynamic parameters from the IC engine working on natural gas at fixed lambda = 1 (stoichiometric combustion), at speed of n = 1250 rpm and fixed load expressed by IMEP in the range in between 475-481 kPa.
The following conclusions were worked out:
– lower peak combustion pressure with higher overlap. It is observed for the entire pressure trace including compression stroke. Thus, one can conclude, that it goes with lower amounts of gases trapped in the cylinder at intake valve closure,
– higher maximum in HRR was observed with bigger overlap. It also affects duration of both combustion phases: CA0-10 and CA10-90, makes them both shortened from 45 to 35 CA deg.
– CA10-90 is strictly in negative, linear correlation with max. of HRR. This is general correlation that can be also justifiable in tests on other engines,
– both histograms for IMEP and polytropic indexes feature with their normal distribution, that leads to conclusions on their Gaussian random distributions,
– both the polytropic indexes are in light positive correlations, so it might mean either lower exhaust residuals can be found in the engine with increase of overlap or lower heat transfer to cylinder walls, so to a cooling system.

Acknowledgements

References

[1] Szymkowiak, M., Szwaja, S., *New concept of a rocker engine – kinematic analysis*, Journal of KONES Powertrain and Transport, Vol. 19, No. 3, pp. 443-450, 2012.

[2] Racewicz, S., Olejnik, A., *Control of Fiat multiair valve-lift system using Atmega micro-controller*, Journal of KONES Powertrain and Transport, Vol. 24, No. 3, pp. 119-236, 2017.

[3] Sendyka, B., Sochan, A., Noga, M., Rodak, L., *The description of the total efficiency of 2SZ-FE engine with the variable valve timing*, Journal of KONES Powertrain and Transport, Vol. 14, No. 2, pp. 401-407, 2007.

[4] Grab-Rogalinski, K., Szwaja, S., *The combustion properties analysis of various liquid fuels based on crude oil and renewables*, IOP Conference Series: Materials Science and Engineering, IOP Conf. Ser.: Mater. Sci. Eng., 148, 012066, 2016.

[5] Szwaja, S., Ansari, E., Rao, S., Szwaja, M., Grab-Rogalinski, K., Naber, J. D., Pyrc, M., *Influence of exhaust residuals on combustion phases, exhaust toxic emission and fuel consumption from a natural gas fueled spark-ignition engine*, Energy Conversion and Management, Vol. 165, pp. 440-446, 2018.

[6] Szwaja, S., Naber, J. D., *Exhaust gas recirculation strategy in the hydrogen SI engine*, Journal of KONES Powertrain and Transport, Vol. 14, No. 2, pp. 457-464, 2007.

[7] Szwaja, S., Naber, J. D., *Impact of leaning hydrogen-air mixtures on engine combustion knock*, Journal of KONES Powertrain and Transport, Vol. 15, No. 2, pp. 483-492, 2008.